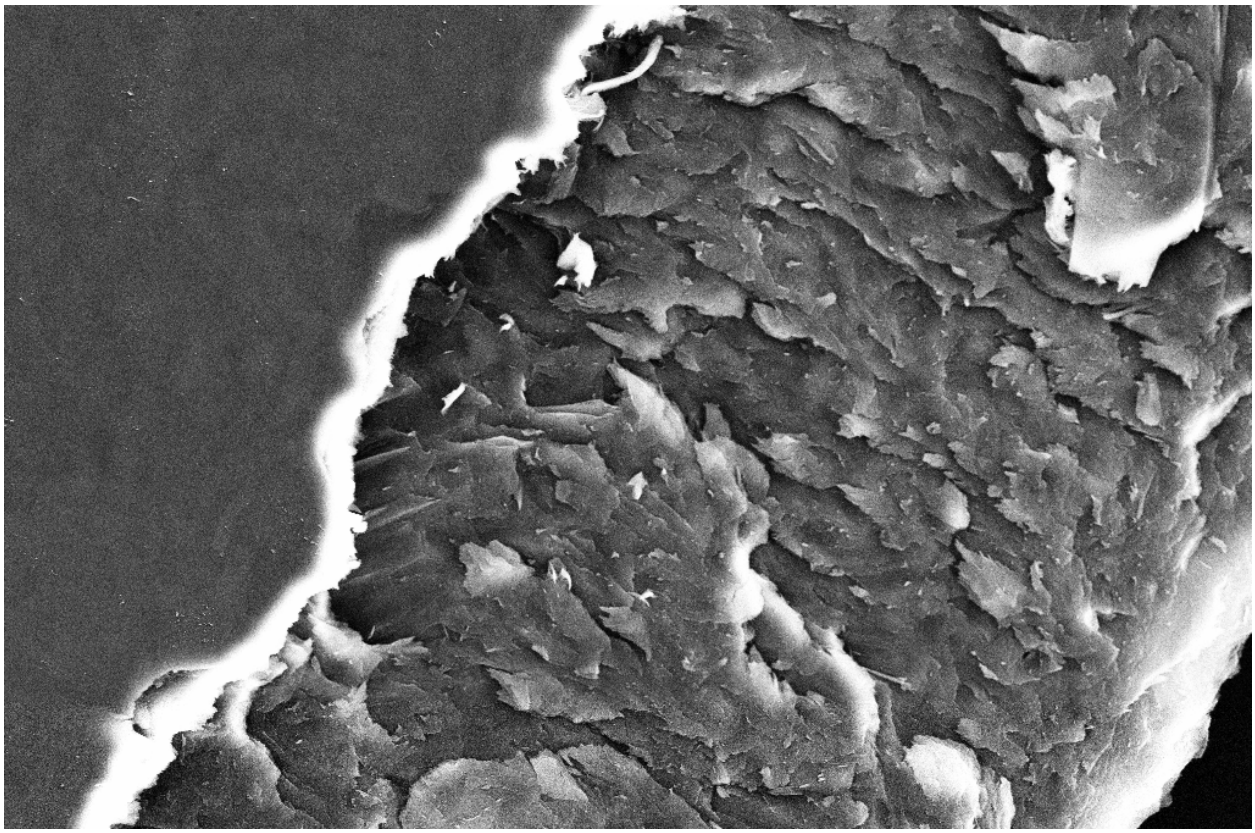

The Enzymatic Desulfation of Cellulose Nanocrystals using Sulfatase

Master's thesis in Biotechnology

ELIN HORN

DEPARTMENT OF CHEMISTRY AND CHEMICAL ENGINEERING

CHALMERS UNIVERSITY OF TECHNOLOGY
Gothenburg, Sweden 2024
www.chalmers.se

Master's thesis

The Enzymatic Desulfation of Cellulose Nanocrystals using Sulfatase

ELIN HORN

CHALMERS
UNIVERSITY OF TECHNOLOGY

Department of Chemistry and Chemical Engineering
Division of Organic Chemistry
Gunnar Westman´s research group
Chalmers University of Technology
Gothenburg, Sweden 2024

The Enzymatic Desulfation of Cellulose Nanocrystals using Sulfatase
ELIN HORN

Supervisor: Jelka Feldhusen, Division of Chemistry and Biochemistry, Chalmers University of Technology
Examiner: Gunnar Westman, Division of Chemistry and Biochemistry, Chalmers University of Technology

Master's Thesis 2024
Department of Chemistry and Chemical engineering
Chalmers University of Technology
SE-412 96 Gothenburg
Telephone +46 31 772 1000

Cover: SEM image of a CNC film, cast after treatment with sulfatase and buffer solution.

Typeset in LaTeX
Printed by Chalmers Reproservice
Gothenburg, Sweden 2024

The Enzymatic Desulfation of Cellulose Nanocrystals using Sulfatase
ELIN HORN
Department of Chemistry and Chemical engineering
Chalmers University of Technology

Abstract

Through sulfuric acid hydrolysis of cellulose, cellulose nanocrystals (CNCs) can be obtained, with sulfate half-ester groups at the surface. Substantial research have been dedicated to chemically modify the hydroxyl groups present on the CNC surface to alter their chemical and mechanical properties. Another approach involves the desulfation of CNCs, and thereby increase the availability of the surface hydroxyl groups. In this project the enzyme sulfatase extracted from the snail *Helix pomatia*, was used to catalyze the hydrolysis of the sulfate half-ester on the CNC surface. To monitor the activity and inhibition of sulfatase UV-Vis spectroscopy was employed. A protocol for sulfate determination of CNC after treatment with sulfatase and buffer solution was developed, where CNC dispersed in Acetate buffer resulted in enzymatic desulfation. The sulfate content on the CNC surface was measured using conductometric titration and dry weight determination after CNC had been hydrolysed for various amount of time. CNC films were cast after hydrolysis and applied in characterization using FT-IR and SEM.

Keywords: Nanocellulose, enzymatic hydrolysis, desulfation, surface modification, films.

Acknowledgements

To Gunnar, thank you for sharing your knowledge and teaching me so much about how to think and what to consider when you are working on a project like this. Thank you for being like a mentor to me, I deeply appreciate your guidance. In addition, I am grateful and excited that we will continue to work together during my doctoral studies.

Thank you Jelka for all the great times both in- and outside the lab and for drilling us master students like a wannabe German drill sergeant. I also want to thank you for sharing your epic dance moves, always cheering me up. Gabriel, I have truly enjoyed working with you and I am going to miss doing the dishes together. I want to thank everyone in the Westman group, it has been a pleasure and an honor to be a part of the group.

A big thanks to all the co-workers at the 9^{th} floor for being so welcoming and kind and for the nice Friday fika, and a special thanks to Ishan for the spectroscopy discussions.

Elin Horn, Gothenburg, June 2024

List of Abbreviations

Abbreviations that have been used throughout the thesis is listed below.

CNC	Cellulose nanocrystals
DI water	Deionized water
DMSO	Dimethyl sulfoxide
EtOH	Etanol
HCl	Hydrochloric acid
MCC	Microcrystalline cellulose
NaCl	Sodium chloride
p-NP	p-Nitrophenol
p-NPS	p-Nitrophenyl sulfate
RT	Room temperature

List of Equipment

Equipment used in the project and their location is listed below.

Conductometric titration	888 Titrando and the 801 Stirrer (Metrohm) located in room 9058 at the 9^{th} floor in the chemistry building.
Data processing	RStudio version 4.2.2 with installed packages tidyverse and ggplot2.
FT-IR Spectroscopy	Hyperion3000/Vertex70v (Bruker) located in room F4112 at Chalmers Materials Analysis Laboratory (CMAL).
SEM	Ultra 55 FEG-SEM (LEO) situated in room F4306 at Chalmers Materials Analysis Laboratory (CMAL).
UV-Vis Spectroscopy	Cary 3500 UV-Vis Multicell Spectrophotometer in lab 5041 at the 5^{th} floor in the chemistry building.

Contents

List of Figures

List of Tables

1

Introduction

Cellulose is often stated as the most abundant biopolymer in the world and can be extracted from e.g wood and cotton [1]. Cellulose is composed of unbranched nanofibers of linear β-1,4-linked glucopyranose units and is the main structural component in the wood cell walls, forming a highly organized hierarchical structure extending from nano- to macroscale in a matrix together with hemicellulose and lignin [2]. In recent years cellulose has gained attention due to its unique properties, including high mechanical strength and stiffness, low density and toxicity and large surface area. These properties make cellulose attractive for use in several hybrid materials [3]. Cellulose nanocrystals (CNCs) can be obtained through sulfuric acid hydrolysis of cellulose, where anionic sulfate half-ester groups replaces some hydroxyl groups at the surface [4], see Figure 1.1. Nanocrystals from acid-hydrolysed cellulose have been of specific interests since it was demonstrated that they could form chiral nematic phases in suspension, resembling the highly textured organizations of microfibrils found in nature. CNCs of various morphologies can be prepared by altering the cellulose source and hydrolysis conditions. Through the usages of transmission electron microscopy, flow birefringence, and viscometry it has been concluded that CNCs are generally elongated and flat, ca 200 nm long, 10-20 nm wide and a few nm thick [5]. The repulsion between their negatively charged surfaces control CNCs' stability in water and their chiral nematic liquid crystal self-assembly and rheological behaviour [4].

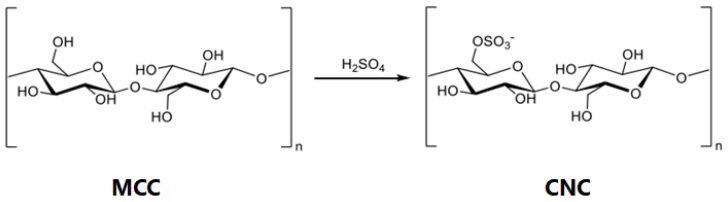

Figure 1.1: The structure of microcrystalline cellulose (MCC), that upon sulfuric acid hydrolysis results in cellulose nanocrystals (CNC) with sulfate groups on the surface.

Considerable research have been dedicated to chemically modify the hydroxyl groups present on the CNC surface to alter their chemical and mechanical properties, making them more versatile. CNCs have high surface-to-volume ratios and several hydroxyl groups that can be used for surface functionalizations [2]. Through surface modifications CNCs can be utilized in various fields including biomedicine, pharmceuticals, electronics, barrier films, nanocomposites and more [6]. An alternative

approach involves the desulfation of CNCs, which thereby increase the availability of the surface hydroxyl groups. Desulfation is the process where sulfate half-ester groups are hydrolysed, leading to a reduction in surface charge that can destabilize aqueous CNC dispersions [7]. Below a certain surface charge density attractive van der Waals forces dominates and the CNCs will agglomerate or precipitate. Various chemical methods for desulfation have been reported, including acidic, solvolytic and alkaline desulfation. Desulfation kinetics are slow at RT even in concentrated acidic H-CNC solutions and it seems as though high concentrations of acid or base and an elevated temperature is needed to accelerate the hydrolysis reaction. A problem with these chemical methods is that addition of a strong acid or base may increase the risk of depolymerization [4]. Therefore another method for a controllable desulfation on the CNC surface is needed. In this project an enzymatic method is evaluated to gain insight of the desulfation kinetics on the CNC surface. Sulfatase extraced from *Helix pomatia* is the enzyme used, with the function to catalyze the hydrolysis of sulfate esters.

1.1 Project objective

The aim of the thesis is to examine to what extent sulfatase can effectively hydrolyse sulfate groups on CNC and how these surface modifications affect the properties of CNC. Further, the objective of the project is to do the following:

i Develop a protocol for sulfate determination on the CNC surface after treatment with a buffer solution.

ii Determine the reactivity of sulfatase on CNC.

iii Analyse how the CNC surface is altered upon enzymatic hydrolysis and how the chemical properties change.

1.2 Specification of the issue being investigated

Indications from chemical hydrolysis of sulfate groups on the CNC surface implies that there are two desulfation reactivities, one fast reactivity and one that is slower [4]. To utilize the difference in reactivities is difficult when chemical methods are applied, but might be possible with enzymatic methods, see Figure 1.2. In addition, sulfatase should be solved in a buffer solution for controllable activity and therefore the CNC will be suspended in buffer before hydrolysis. The thesis aims to investigate how various buffers may affect the CNC surface by coordination to the sulfate groups.

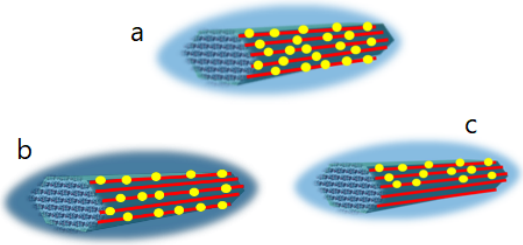

Figure 1.2: (a) shows the hexagonal cross section of CNC, where the yellow dots represents sulfate groups on the surface. (b) represents the CNC surface after chemical hydrolysis, resulting in a randomized desulfation pattern. (c) shows a selective desulfation pattern and how the CNC surface potentially could look after enzymatic methods have been applied.

Figure 1.3 can be employed to further understand why enzymatic methods could lead to a selective desulfation. In Figure 1.3 the sulfate groups are oriented downwards, indicated by the orange arrows. In the crystallites the sulfate groups are in close proximity to the next layer of β-1,4-linked glucopyranose. However, an acid or base used in chemical hydrolysis can still penetrate through and desulfate these sulfate groups. An enzyme, on the other hand, might be too big to reach these sulfate groups, while still being able to hydrolyse the sulfate groups furthest away, resulting in a selective desulfation.

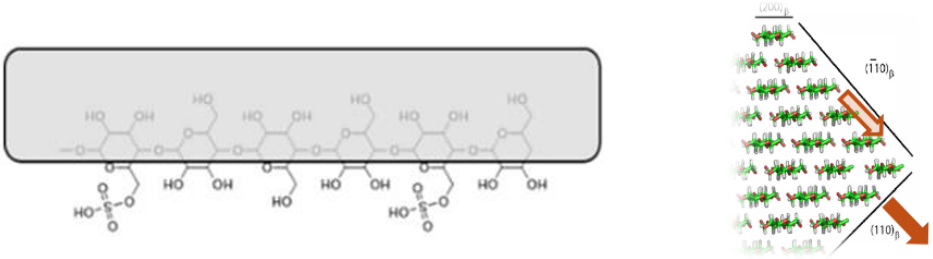

Figure 1.3: Orientation of sulfate groups on the CNC surface. To the right the crystal structure of cellulose is displyed, highlighting two of the lattice planes.

2

Theory

Sulfatases are enzymes that catalyze the hydrolysis of sulfate esters to their corresponding alcohols. They hydrolyse a wide range of sulfate ester substrates, from hydrophobic steroids, to amphiphilic sulfated carbohydrates and glycolipids and hydrophilic mono- and disaccharide sulfates [8]. Sulfatases have a highly conserved sequence and structure across eukaryotic and prokaryotic species. Eukaryotic cells are characterized by the presence of a nucleus, whereas prokaryotic cells lack a nucleus. Similarities shared by sulfatases are 20-60% sequence homology over the entire protein length, a highly conserved N-terminal and a unique active-site aldehyde residue, α-formylglycine (FGly). Sulfatases are generally between 500 and 600 amino acids in length. Their active site constitutes of ten interlinked polar residues and a divalent metal cation which has been determined through studies in crystallography and mutagenesis, see Figure 2.1 [13]. Numerous sulfatases in various organisms have been identified. However, in the thesis sulfatase from the snail *Helix pomatia* was employed. Sulfatase from *Helix pomatia* is commercially available as a crude powder and has been used in research involving doping control and metabolomics due to its promiscuity. However, the *Helix pomatia* extract also contain other enzymes, such as β-glucuronidase and the sulfatase specificity may be hindered due to these impurities [10].

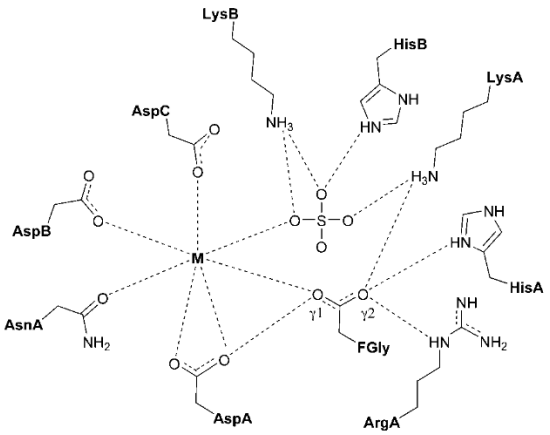

Figure 2.1: Overview of the conserved residues within the active site of sulfatase [13].

2.1 Proposed mechanism of action

In Figure 2.2 the proposed mechanism of action is displayed, involving FGly and key active-site residues based on the crystal structure and mutagenesis. It has not been concluded whether the transition state of sulfate ester hydrolysis is primarily associative (S_N2-like) or dissociative (S_N1-like) [13].

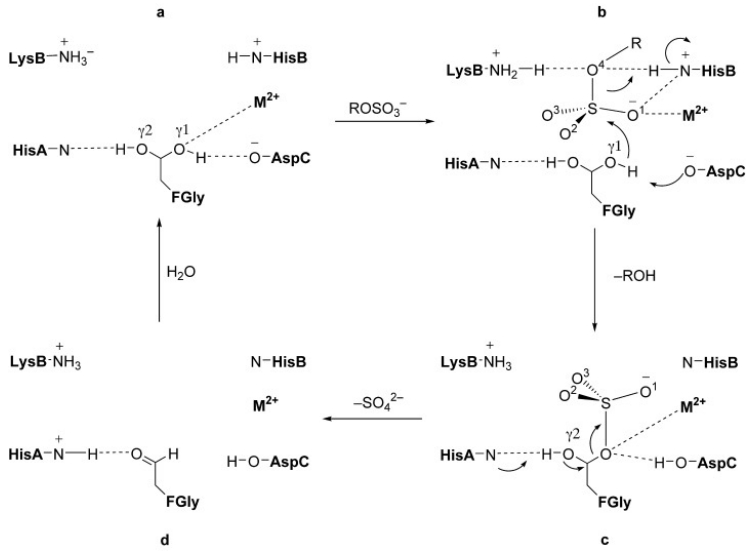

Figure 2.2: Proposed mechanism of the sulfatase hydrolysis reaction [13].

2.2 Enzymatic hydrolysis

The sulfatase activity is dependent on buffer pH and temperature, see Figure 2.3. Zhao, K. et al. reported that at temperatures between 25-45 °C sulfatase from *Helix pomatia* will have a high and stable activity. Even when the temperature was lowered to 4 °C 53.2% of the activity remained. However, the sulfatase activity continuously decreased after 35 °C, to 2.5% at 75 °C [9].

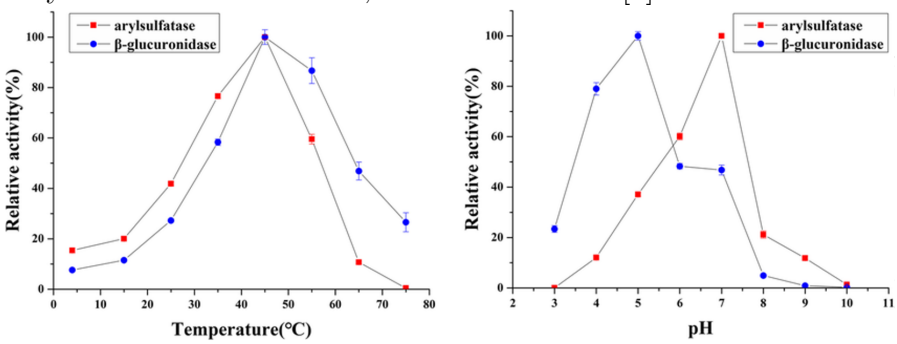

Figure 2.3: Sulfatase activity dependence of temperature and pH [9].

3

Characterisation techniques

3.1 Nuclear magnetic resonance spectroscopy

Nuclear magnetic resonance (NMR) spectroscopy is based on the magnetic properties of the nuclei of atoms. Subatomic particles can be visualized as spinning around their axis. Due to the movement of charge, the nucleus generates a magnetic dipole along the direction of the spin axis. Nuclei with an odd mass or atomic number, such as ^{1}H and ^{13}, have a nuclear spin quantum number. When a magnetic field is applied a nucleus with a spin I adopts 2I + I orientation. Each orientation correlates to an energy level that is designated a magnetic quantum number, m (m = -I to +I). Irradiation with microwaves (MHz) of a sample in a magnetic field leads to energy absorbtion of the nuclei, which changes the orientation of the nuclear spins from a low-energy spin state to a high-energy spin state. The energy absorption occurs when the frequency of radiation is in resonance with the applied magnetic field. This energy is recorded to acquire the specific fingerprint spectra of a given molecule [14].

3.2 UV-Vis spectroscopy

Ultra Violet-Visible (UV-Vis) spectrophotometers measure the absorption or transmission of light that passes through a medium as a function of wavelength [15]. Many materials contain chromophores, which are molecules that absorb ultra violet or visible light at particular wavelengths. The Lambert-Beer's law relates the absorption of a sample at a given wavelength to the sample concentration.
The Lambert-Beer's law is given by:

$$A = \varepsilon \cdot c \cdot l \tag{3.1}$$

Where A is the absorbance, ε is the molar absorptivity, c is the concentration of the solute and l is the path length of the cuvette [16].

3.3 Conductometric titration

Conductometric titration is a commonly used method for surface-charge determination. The technique can be employed to distinguish the different surface groups and their contribution to electrical stability. Upon conductometric titration of latices or colloids, the surface and the structure of the double layer should be considered, since

the interpretation of these results may not be as straight forward as conductometric titration of free acid [17].

$$Sulfate\ (\mu mol/g) = \frac{V_{NaOH}[NaOH]}{m_{CNC}M_s} \times 10 \tag{3.2}$$

Where V_{NaOH} is the added volume NaOH at the equivalence point, [NaOH] is the concentration of the titrant, m_{CNC} is the dry weight CNC and M_s is the mass of the suspension being titrated [18].

3.4 Fourier transform infrared spectroscopy

Fourier transform infrared (FT-IR) spectroscopy utilizes the adsorption of light in the infrared region. The resulting spectrum can be viewed as a molecular fingerprint of the sample where the absorption peaks correspond to the frequencies of vibrations between the bonds of the atoms constituting a sample. By analysing the peaks identification of different components can be made and through measurement of the peak size the amount of material can be determined [19].

3.5 Scanning electron microscopy

The principle behind scanning electron microscopy (SEM) is that an electron beam is aimed at a sample to form a magnified image of the material. When electrons are applied to a sample they interact with said sample, generating secondary electrons, backscattered electrons, transmitted electrons and characteristic X-rays, which can be captured to generate images. SEMs can be operated in various modes to detect different electrons. Using a conventional SEM, the sample has to be conductive or coated with a thin layer of gold or platinum to ensure conductivity, otherwise the electrons will not interact with the sample and no image will be created [20]. If samples of high humidity is to be studied, environmental Scanning electron microscopy (ESEM) can be used since this technique do not require high vacuum or a conductive sample. The resolution is however not as high for ESEM (3.5-5.0 nm) as for SEM (5.0-10.0 nm) [21].

4

Experimental

The experimental procedures are listed below. For preparation of Tris buffer Tris base (tris(hydroxymethyl)aminomethane) was solved in DI water and concentrated HCl was added to adjust the buffer pH. In preparation of Acetate buffer Sodium Acetate was solved in DI water and Acetic aced was utilized for adjustment of the pH.

4.1 Synthesis of p-Nitrophenyl sulfate (p-NPS)

To 5 ml carbon disulfide N,N-dimethylaniline (4.7 ml, 37 mmol) and chlorosulfonic acid (0.9 ml, 14 mmol) was added. The suspension was stirred for 5 min (RT) and p-Nitrophenol (1.4 g, 10 mmol) was slowly added. The resulting slurry was heated (50 °C) and stirred for 90 min. Thereafter, the temperature was lowered (25 °C) and the reaction was stirred overnight. The suspension was cooled on ice. 20 ml of 4 M KOH was carefully added and the stirring was continued for another 30 min. Afterwards, the slurry was filtered and warm water was added for recrystallization. The resulting crystals was characterised using NMR. ^{1}H NMR (600 MHz, DMSO-d_6): δ 7.40 (d, J=9.24 Hz, 2H), 8.20 (d, J=9.24 Hz, 2H). ^{13}C NMR (600 MHz, DMSO-d_6): δ 125.6 (2xC) 120.1 (2xC).

4.2 UV-Vis measurements

To obtain an absorbance value of ca 0.9 the Lambert-Beer's law was used in preparation of the UV-Vis spectroscopy measurements, see Equation 3.1. The cuvette path length was 1 cm and p-Nitrophenyl sulfate has a molar absorptivity of 17500 L mol^{-1} cm^{-1}, resulting in a concentration of 51.43 µM. p-Nitrophenyl sulfate (0.001 g, 4.6 µmol) was added to 88 ml Tris buffer and agitated. To an aliquot of 10 ml Tris buffer sulfatase (0.01 g, 20-40 U/ml) was added. 3 ml of p-Nitrophenyl sulfate in Tris was added in a quartz cuvette and a reference specrtum was measured. 1 ml of solution in the cuvette was removed and replaced by 1 ml of the sulfatase in Tris mixture. A new spectra was recorded every 5 minutes for 2 h.

4.3 Enzyme assay

Sulfatase from *Helix pomatia*, Type H-1, sulfatase ≥10,000 units/g solid, was used without further purification. Sulfatase (0.01 g, 20-40 U/ml) was dissolved in 10 ml

Tris buffer or Acetate buffer.

4.4 Resuspension of CNC in buffer

CNC of 1 wt% in aqueous solution was centrifuged at 4300 rpm for 8 min in RT. The supernatant was decanted and the CNC was re-suspended in Tris or Acetate buffer. To replace the water surrounding the CNC with buffer solution, the suspension was centrifuged, decanted and re-dispersed in buffer solution for a total of three times.

4.5 Hydrolysis reaction of CNC in Tris

A time study was conducted where a stock solution of 270 ml CNC in 0.5 M Tris of pH 7.4 was hydrolysed using sulfatase. The suspension was magnetically stirred at 400 rpm at 37 °C. Aliquots of 60 ml were taken after 0 min (before sulfatase was added), 30 min, 120 min and overnight. 30 ml enzyme suspension was added (10 ml for each for each aliquot). A reference suspension without sulfatase was also stirred at 400 rpm at 37 °C to monitor the autohydrolysis. After hydrolysis, the suspensions were heated at 80 °C for 5 min, to inhibit the enzyme. However the same procedure was performed for all samples. Thereafter, the suspensions were cooled on ice to stop the hydrolysis and 1 M HCl was added to reach a pH of ≈2. The suspensions were protonated to remove the Tris base from the sulfate groups. The solutions were transferred to dialysis tubes of membrane size 3.5 kDa and dialysed against DI water until the conductivity was <5 μS. Thereafter, the suspensions were transferred to a beaker containing a magnetic stirrer and 0.6 g Dowex ion exchange resin was added and stirred overnight. The resins were filtered off and the resulting solutions were prepared for titration and dry weight determination.

4.6 Inhibition systems

To evaluate the potential desulfation of CNC during enzyme inhibition three control reactions were performed. In the first one, which was used as a reference, 20 ml 1 wt% CNC was put on dialysis against DI water with a pore membrane of size 3.5 kDa. In the second, 30 ml 1 wt% CNC was diluted in 70 v/v% EtOH (21 ml) and stirred. The mixture was centrifuged once for 8 min at 4300 rpm with a deacceleration speed of 5. The supernatant, being water and ethanol was decanted and the CNC was re-suspended in DI water to a volume of 30 ml. Thereafter the suspension was put on dialysis against DI water. For the third reaction, 30 ml 1 wt% CNC was warmed at 80 °C for 5 min and cooled on an ice bath. The suspension was put on dialysis against DI water.

4.7 Sample preparation

4.7.1 Titration

Titrations were performed in triplicates of 15 ml. To each solution 40 μL of 0.5 M NaCl was added to ensure conductivity. The suspensions were sonicated for 30 s and 23 μL of 1 M HCl was added for protonation of the sulfate groups, resulting in pH$\approx$2.9.

4.7.2 Dry weight determination

Dry weight determination were done in triplicates. Three glass petri dishes were washed with soap and water and left in the oven at 100 °C overnight. The petri dishes were left to cool down (RT) and were weighed three times and the mean value was used. Thereafter, $\approx$5 g of CNC solution was added to each petri dish and they were put in the oven at 50 °C overnight. The petri dishes cooled down and weighed and the dry weights were calculated.

4.7.3 Film casting for SEM

Glass petri dishes were washed and dried in the oven at 100 °C overnight. To each petri dish 20 ml of CNC suspension was added and dried in oven at 50 °C overnight. A small piece of every film was placed on carbon tape and the samples was sputter coated with a 5.13 nm layer gold.

5

Results and discussion

5.1 Activity and inhibition of Sulfatase

To measure and monitor the activity of sulfatase p-Nitrophenyl sulfate was synthesized and characterised using NMR, see Figure A.1 and Figure A.2 for obtained spectrum.

5.1.1 UV-Vis measurements of p-NPS in Tris

The sulfatase activity was monitored using UV-Vis spectroscopy measuring the release of p-Nitrophenol (p-NP) from p-Nitrophenyl sulfate (p-NPS). p-NPS has an absorbance peak at around the wavelength 280 nm. Upon hydrolysis the absorbance peak is shifted to a wavelength of ca 410, corresponding to p-NP [11]. The enzyme activity was monitored for 120 min, where an initial reference spectrum at 0 min (t0) containing p-NPS in Tris buffer was recorded before the enzyme solution (sulfatase in Tris buffer) was added. From there on a new spectra was recorded every 5 minutes for 2 h (t5-t120), see Figure 5.1.

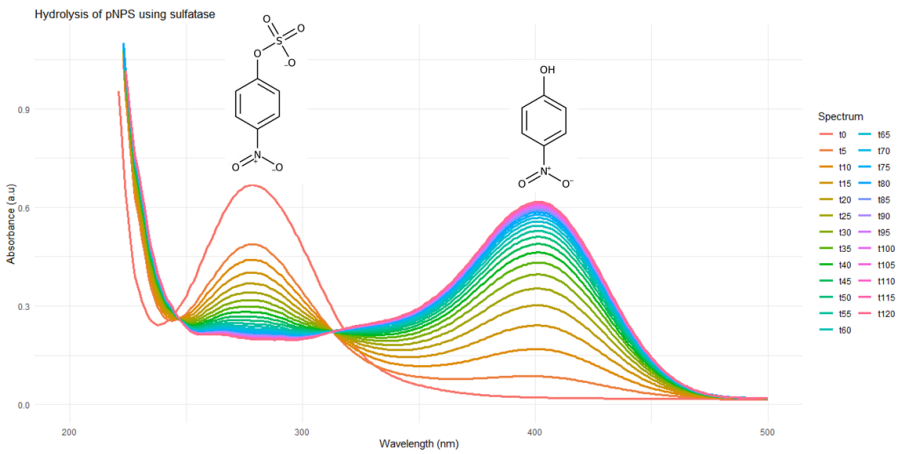

Figure 5.1: UV-Vis measurement of p-Nitrophenyl sulfate and sulfatase in 0.5 M Tris (pH 7.4), with a new spectra recorded every 5 minutes for 2 h (t0-t120).

To be able to monitor the hydrolysis reaction on the CNC surface, it was important to have a way of inhibiting the enzyme. A method where the suspension was heated at 80 °C for 5 min was tested. An initial reference spectrum at 0 min (t0) containing

p-NPS in Tris buffer was recorded before the enzyme solution (sulfatase in Tris buffer) was added, see Figure 5.2.

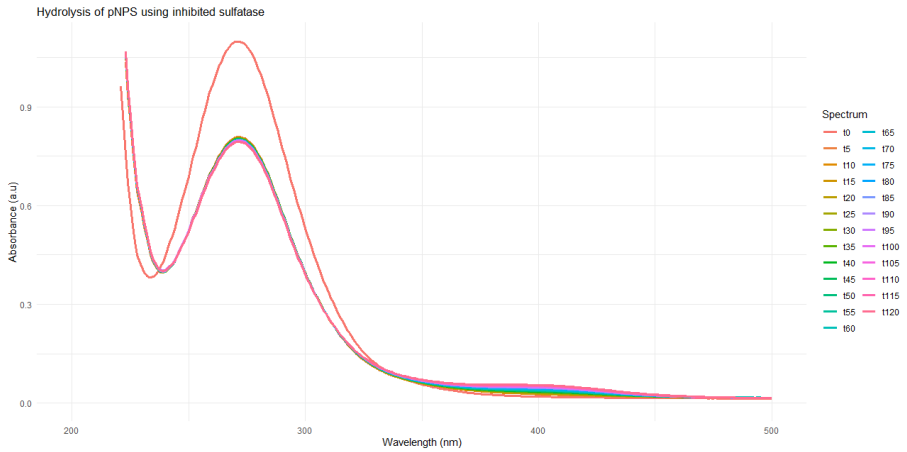

Figure 5.2: UV-Vis measurement of p-Nitrophenyl sulfate and sulfatase in 0.5 M Tris after heating.

A small increase in the absorbance is visible at wavelength 410 nm, indicating some hydrolysis of p-NPS to p-NP. However, in comparison to the absorbance at wavelength 410 nm when the enzyme was not heated, Figure 5.1 this is minor. Therefore, the sulfatase activity can be seen as negligible in Tris buffer after warming at 80 °C for 5 min.

5.2 Enzymatic hydrolysis of CNC in Tris

CNC was centrifuged and resuspended in 0.5 M Tris buffer. From the stock solution of CNC in Tris buffer an initial aliquot was drawn prior to hydrolysis. Thereafter hydrolysis reactions at 37 °C were performed. Aliquots of the stock solution was taken after 30, 120 min and overnight. In addition, a reaction without sulfatase monitoring the autohydrolysis was performed. After centrifugation and dialysis for removal of Tris buffer the suspensions were titrated against 0.01 M NaOH for determination of the sulfate content on the CNC surface. The titration curves are displayed in Figure 5.3, where 0 min* is the initial suspension before hydrolysis, 30 min, 120 min and Overnight are the suspensions where sulfatase was added, and Ref* overnight is the solution used to monitor the autohydrolysis.

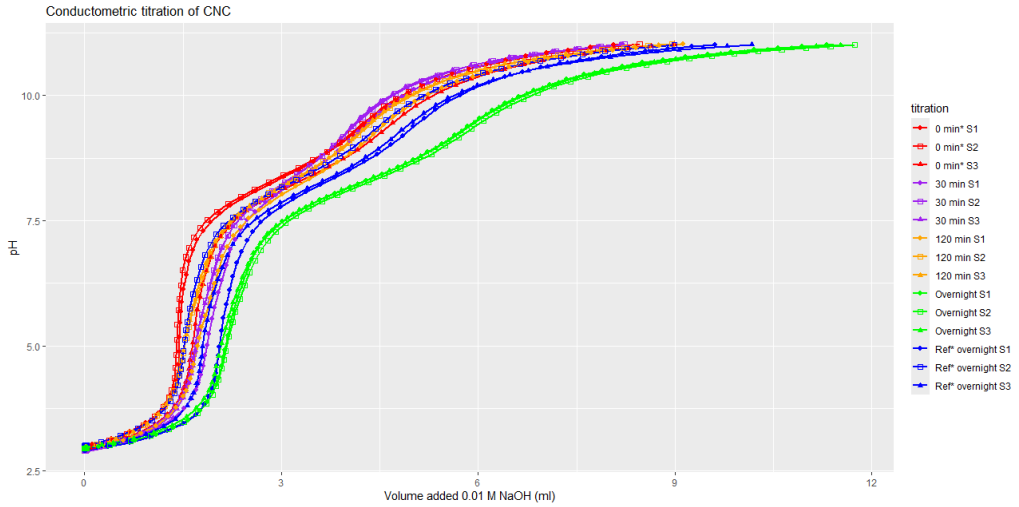

Figure 5.3: Titration of CNC treated with sulfatase and 0.5 M Tris buffer. *indicates that sulfatase has not been added to the suspension.

From each titration the equivalence points were obtained (ERC 1 and ERC 2) and the volume of added NaOH at ERC 1 and ERC 2 was used together with the dry weight content to calculate the sulfate on the CNC surface, see Equation 3.2 and Table 5.1.

Table 5.1: Dry weight and sulfate content of CNC hydrolysed with sulfatase at 37 °C for different periods of times; 0 min, 30 min, 120 min and overnight. *indicates that sulfatase has not been added to the suspension.

Sample	**Dry weight (wt%)**	**Sulfate ERC 1 (μmol/g)**	**Sulfate ERC 2 (μmol/g)**
T0*	0.6216	160.07	470.90
T30 sulf	0.4552	254.56	594.46
T120 sulf	0.6050	171.74	470.51
To/n sulf	0.7822	180.03	496.45
To/n ref*	0.6493	182.30	494.38

The obtained sulfate values for ERC 1 and ERC 2 indicates that sulfatase does not hydrolyse sulfate on the CNC surface since the initial values (T0*) are lower than after treatment with sulfatase. Additionally, the fact that the ERC 1 and ERC 2 values for each sample is far apart implies that there is still Tris present in the suspensions and that it is Tris being titrated at ERC 2. This suggests a strong coordination of Tris to the CNC surface, potentially blocking sulfatase to perform the enzymatic hydrolysis, see Figure 5.4.

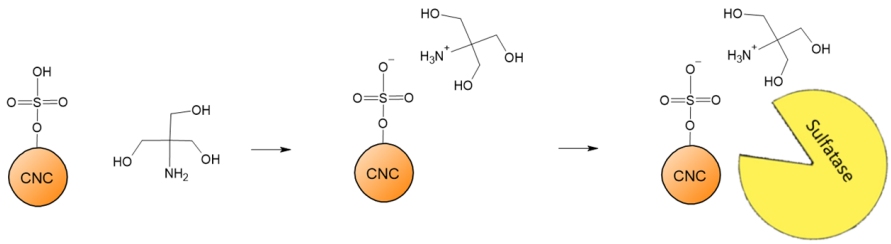

Figure 5.4: Coordination of Tris to sulfate on CNC possibly hinder sulfatase to hydrolyse the CNC.

To decrease the coordination between the sulfate group and Tris buffer 1 M NaOH was added to the aqueous CNC dispersion. This was done to obtain a cationic sodium counterion on the sulfate group and thereby lower the attractive forces between Tris and the sulfate group. After addition of NaOH to CNC the dispersion was centrifuged and resuspended in Tris buffer. From the stock suspension of CNC in Tris buffer an initial aliquot was drawn prior to hydrolysis. Thereafter hydrolysis reactions at 37 °C were performed, one where sulfatase was added and one without sulfatase, to monitor the autohydrolysis. After centrifugation and dialysis for removal of Tris buffer the suspensions were titrated against 0.01 M NaOH for determination of the sulfate content on the CNC surface. The titration curves is displayed in Figure 5.5, where 0 min* is the initial suspension before hydrolysis, Overnight is the suspension where sulfatase was added, and Ref* overnight is the solution used to monitor the autohydrolysis.

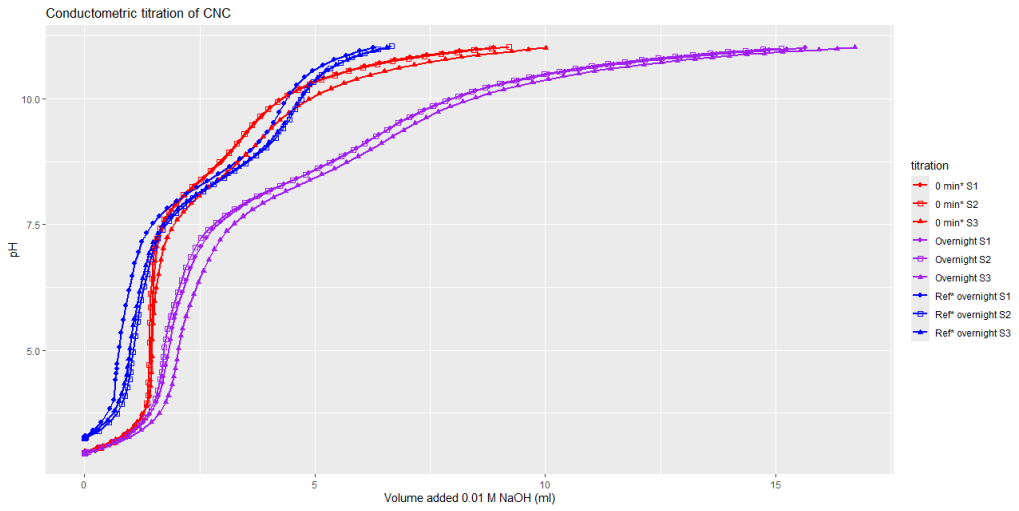

Figure 5.5: Titration of CNC treated with sulfatase and 0.5 M Tris buffer. *indicates that sulfatase has not been added to the suspension.

From the titration curves the equivalence points (ERC 1 and ERC 2) and added volume NaOH at the equivalence points were obtained and used together with the dry weight content for calculation of the sulfate content, see Table 5.2.

Table 5.2: Dry weight and sulfate content for CNC hydrolysed with sulfatase in Tris at 37 °C. *indicates that sulfatase has not been added to the suspension.

Sample	Dry weight (wt%)	Sulfate ERC 1 (μmol/g)	Sulfate ERC 2 (μmol/g)
T0*	0.7739	124.35	302.09
To/n sulf	0.9781	126.56	440.79
To/n ref*	0.9480	73.51	357.60

The obtained sulfate values indicates that there is no enzymatic hydrolysis, since To/n sulf is 126.56 µmol/g compared to 124.35 µmol/g at T0* (prior to hydrolysis) at ERC 1. Likewise, the sulfate content is 440.79 µmol/g for To/n sulf at ERC 2 and 302.09 µmol/g for T0*, which suggests a higher sulfate content after enzymatic hydrolysis. Comparing the sulfate content for To/n ref*, used to monitor the autohydrolysis to T0*, there is a 59.1% decrease in the sulfate content for To/n ref* at ERC 1. However, the sulfate content is higher for To/n ref* compared to T0* at ERC 2, 357.60 µmol/g and 302.09 µmol/g. Additionally, the values calculated for ERC 1 and ERC 2 being so far apart suggest that the Tris buffer has not been entirely removed and that Tris is being measured at ERC 2 instead of sulfate. From this it would seem as if sulfatase can not desulfate CNC or that another buffer system needs to be evaluated.

5.3 Enzymatic hydrolysis of CNC in Acetate

Carrageenan is a sulfated polysaccharide commonly used as food additive. Sulfatase has been reported to desulfate carrageenan in 0.05 M Acetate buffer [12]. UV-vis measurements of p-NPS and sulfatase in 0.05 M Acetate were performed, see Figure A.3 and Figure A.4. The peak shift in Figure A.3 indicate low buffer capacity, altering the spectra as the p-NPS is hydrolysed and the pH is decreased. Figure 5.6 shows an overview of the molecular structure of the sodium acetate and sulfate group on the CNC surface. The structures suggest low coordination, potentially making the sulfate groups accessible to sulfatase for desulfation.

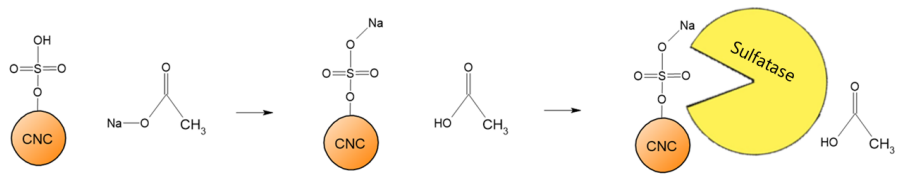

Figure 5.6: Structure of sulfate group on CNC surface and Acetate buffer indicating low coordination, making it possible for sulfatase to bind to, and desulfate CNC.

5.3.1 UV-Vis measurements of p-NPS in Acetate

The sulfatase activity in Acetate buffer was monitored using UV-Vis spectroscopy measuring the release of p-Nitrophenol (p-NP) at 410 nm from p-Nitrophenyl sulfate (p-NPS) at 280 nm [11]. The enzyme activity was monitored for 120 min, where an initial reference spectrum at 0 min (t0) containing p-NPS in 0.5 M Acetate buffer (pH 6.2) was recorded before the enzyme solution (sulfatase in Acetate buffer) was added. From there on, a new spectrum was recorded every 5 minutes for 2 h (t5-t120), see Figure 5.7.

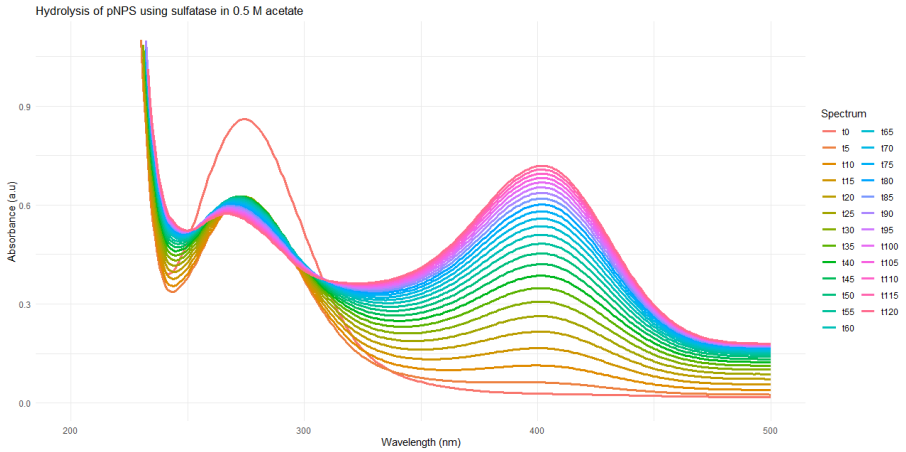

Figure 5.7: UV-Vis measurement of p-Nitrophenyl sulfate and sulfatase in 0.5 M Acetate buffer.

The alteration in the spectra (excluding the peaks) may arise from turbidity/precipitation as the reaction progresses, which can be inferred from the scattering as observed in Figure 5.7 where the initial absorbance values differs from zero, indicating that p-NPS is less soluble in Acetate than Tris buffer. Nonetheless, the same peak shift still occurs as for p-NPS in Tris, meaning that sulfatase has activity in 0.5 M Acetate buffer. UV-Vis measurements was also performed after the enzyme solution had been warmed at 80 °C for 5 min, to evaluate this method of inhibiting sulfatase, see Figure 5.8.

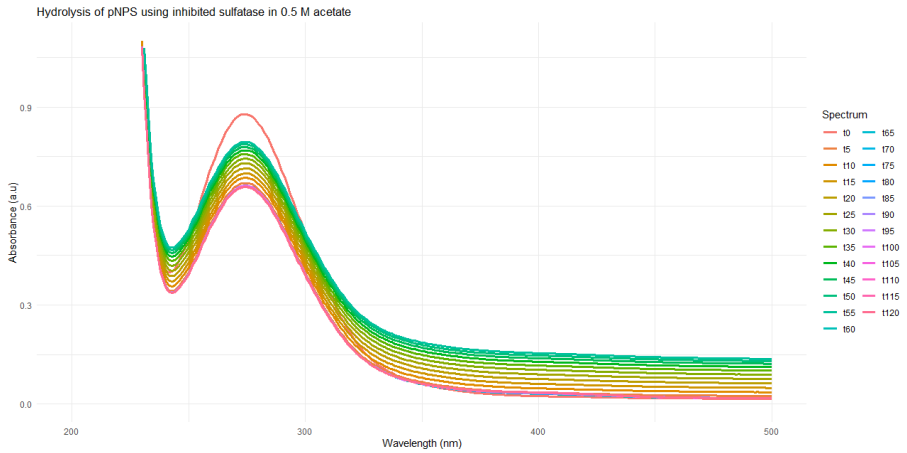

Figure 5.8: UV-Vis measurement of p-Nitrophenyl sulfate and inhibited sulfatase in 0.5 M Acetate buffer.

No peak was observed at wavelength 410 nm, indicating that p-NP was not present in the suspension and thereby that no hydrolysis reaction was taking place. Therefore, warming at 80 °C for 5 min can be used to inhibit sulfatase in Acetate buffer. Additionally, the autohydrolysis of p-NPS in 0.5 M Acetate buffer at 37 °C was measured to ensure the sulfatase activity, see Figure 5.9.

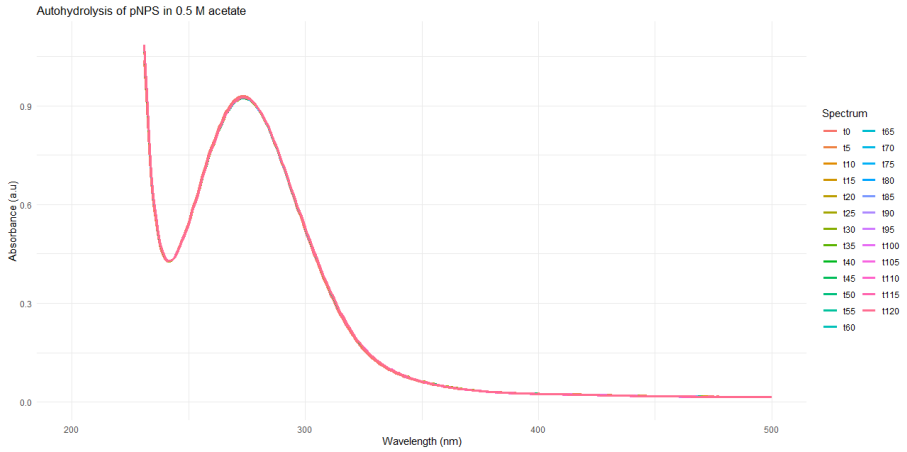

Figure 5.9: UV-Vis measurement of the autohydrolysis of p-Nitrophenyl sulfate in 0.5 M Acetate buffer.

There was no visible shift in the peak, meaning that p-NPS showed no autohydrolysis during the measurement. Therefore, the peak shift and thereby hydrolysis of p-NPS in Figure 5.7 could be attributed to sulfatase.

5.3.2 Sulfate content of CNC in Acetate at 37 °C

CNC was centrifuged and resuspended in 0.5 M Acetate buffer. From the CNC suspension an aliquot was taken prior to hydrolysis. Thereafter hydrolysis reactions at 37 °C were performed, one where sulfatase was added and one without sulfatase, to monitor the autohydrolysis. Afterwards, centrifugation and dialysis was used for

removal of sulfatase ans Acetate buffer. The suspensions were titrated against NaOH for determination of the sulfate content on the CNC surface. The titration curves are shown in Figure 5.10, where 0 min* is the initial suspension before hydrolysis, Overnight is the suspension where sulfatase was added, and Ref* overnight is the solution used to monitor the autohydrolysis. It should be noted that two different batches of titrant were used for the titrations below. For the samples 0 min* and Overnight a titrant of 0.01 M NaOH was used. However, a fresh batch of 0.0115 M NaOH was utilized for Ref* overnight, which explains why these curves are steeper. Looking at the titration curves for T0*, there are some variations and S1 might be an outlier. However, all the samples (S1-S3) have been used to calculate the sulfate content for two reasons. Firstly, being consistent with the data analysis for reproducibility. Secondly, not overestimating the results, since titration curves more to the left in the graph will stand for a lower sulfate content.

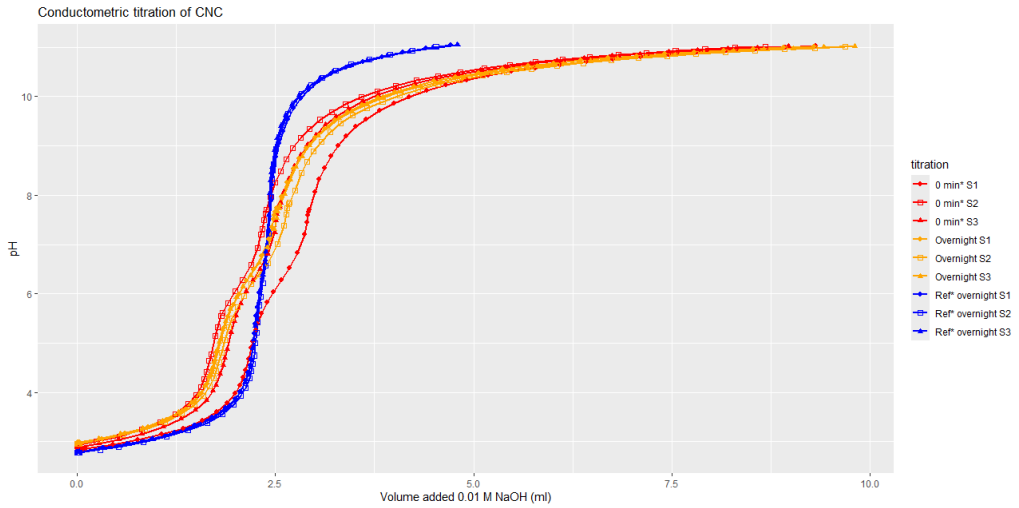

Figure 5.10: Titration of CNC treated with sulfatase and 0.5 M Acetate buffer. *indicates that sulfatase has not been added to the suspension.

From each titration the equivalence points were obtained (ERC 1 and ERC 2) and the volume of added NaOH at ERC 1 and ERC 2 was used together with the dry weight content to calculate the sulfate on the CNC surface, see Table 5.3.

Table 5.3: Dry weight and sulfate content for CNC hydrolysed with sulfatase in Acetate at 37 °C. *indicates that sulfatase has not been added to the suspension.

Sample	**Dry weight (wt%)**	**Sulfate ERC 1 (μmol/g)**	**Sulfate ERC 2 (μmol/g)**
T0*	0.6074	213.46	283.45
To/n sulf	0.8270	143.95	205.17
To/n ref*	0.7601	227.36	246.01

At ERC 1 the sulfate content is lowered by 67.4% from T0* to To/n Sulf, while the

sulfate content, comparing the same suspensions for ERC 2 is lowered with 72.4%. Looking at the sulfate content for To/n ref* in relation to T0*, there is no desulfation at ERC 1 (1.07%) but a 86.8% decrease at ERC 2. Comparing To/n Sulf to To/n ref*, the sample To/n Sulf has a 67.5% percentage points lower sulfate content for ERC 1, whereas To/n ref* has a 14.4 percentage points lower sulfate content at ERC 2. This indicates that the autohydrolysis is more prominent at ERC 2 than the enzymatic hydrolysis. Furthermore, there is no significant autohydrolysis at ERC 1, but a 67.4% enzymatic hydrolysis, which implies that this is the reaction where sulfatase may be advantageous for tuning desulfation on CNC.

5.3.3 Sulfate content of CNC in Acetate at 22 °C

To lower the reactivity of sulfatase and thereby the selectivity on the CNC surface hydrolysis reactions were done at RT. CNC was centrifuged and resuspended in 0.5 M Acetate buffer. From the CNC solution, an aliquot was taken prior to hydrolysis. Thereafter hydrolysis reactions at 22 °C were performed, one where sulfatase was added and one without sulfatase, to monitor the autohydrolysis. Thereafter centrifugation and dialysis were used for removal of sulfatase and Acetate buffer. The suspensions were titrated against 0.0115 M NaOH for determination of the sulfate content on the CNC surface. The titration curves are diplayed in Figure 5.11, where 0 min* is the initial suspension before hydrolysis, Overnight is the suspension where sulfatase was added, and Ref* overnight is the solution used to monitor the autohydrolysis.

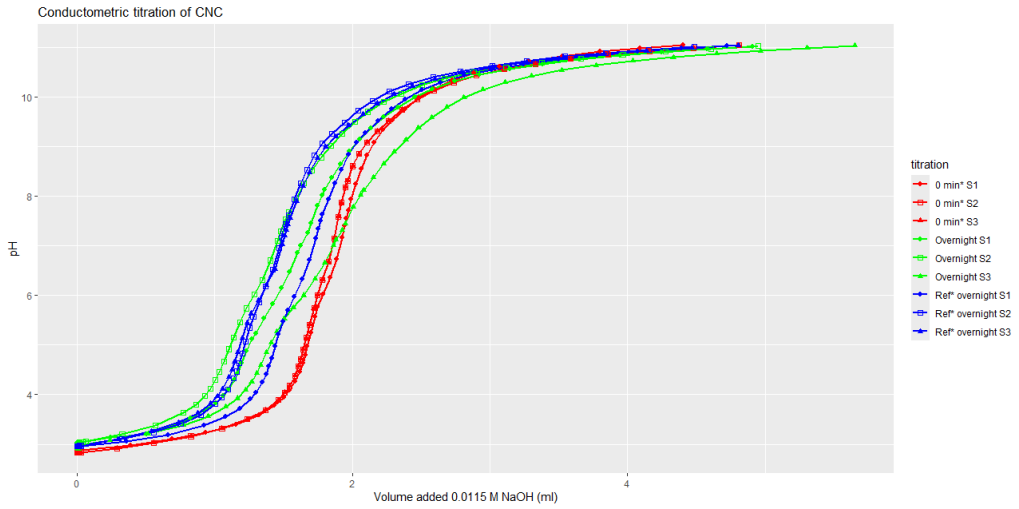

Figure 5.11: Titration of CNC treated with sulfatase and 0.5 M Acetate buffer. *indicates that sulfatase has not been added to the suspension.

From each titration the equivalence points were obtained (ERC 1 and ERC 2) and the volume of added NaOH at ERC 1 and ERC 2 was used together with the dry weight content to calculate the sulfate on the CNC surface, see Table 5.4.

Table 5.4: Dry weight and sulfate content for CNC hydrolysed with sulfatase in Acetate at 22 °C. *indicates that sulfatase has not been added to the suspension.

Sample	Dry weight (wt%)	Sulfate ERC 1 (μmol/g)	Sulfate ERC 2 (μmol/g)	Sulfate ERC 3 (μmol/g)
T0*	0.7505	213.25	245.59	-
To/n sulf	0.7670	153.27	204.99	228.09
To/n ref*	0.8117	149.86	186.01	-

At ERC 1 the sulfate content is lowered by 71.9% comparing To/n Sulf to T0*, while there is 83.5% decrease in sulfate content at ERC 2. Comparing these values to the once earlier obtained during hydrolysis reaction at 37 °C, there was a decrease of 67.4% and 72.4% for ERC 1 and ERC 2 respectively. This would indicate that sulfatase has a higher activity on the CNC surface for both sulfate reactivities when the reaction temperature is lowered to room temperature (22 °C). However, looking at the values obtained for the reference sample, To/n ref*, the sulfate content has decreased by 70.3% and 75.7% at ERC 1 and ERC 2 respectively. This means that sulfatase increases the desulfation by 1.6 percentage point for ERC 1 and 7.8 percentage point at ERC 2. The higher extent of autohydrolysis can be explained by usages of a buffer of higher pH (≈7) leading to alkaline desulfation, especially since the autohydrolysis was not dominant when the hydrolysis was done at 37 °C and at pH 6.2, see Table 5.3. The presence of three ERC values for dispersion To/n sulf could indicate that sulfatase has not been completely removed and is measured at the last equivalence point (ERC 3).

5.3.4 Sulfatase inhibition systems

Two methods that have been reported for the inhibition of sulfatase were applied to CNC in aqueous solution to evaluate if the methods themselves could desulfate CNC. One of the methods was heating at 80 °C for 5 min and the other was to add 70 v/v% EtOH to inhibit the enzyme. After the methods had been employed the CNC suspensions were titrated and their dry weight were determined, a reference of CNC in milli-q was also evaluated, see Figure 5.12.

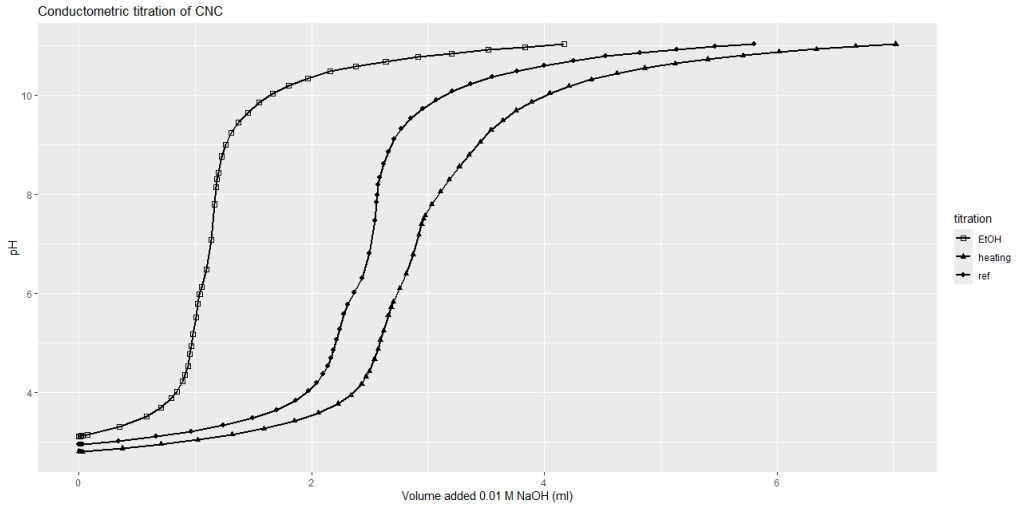

Figure 5.12: Titration of CNC suspensions after diffrent ways of inhibition.

From each titration the equivalence points were obtained (ERC 1 and ERC 2) and the volume of added NaOH at ERC 1 and ERC 2 was used together with the dry weight content to calculate the sulfate on the CNC surface, see Table 5.5.

Table 5.5: Dry weight and sulfate content for CNC determined after different enzyme inhibition system were applied.

Sample	**Dry weight (wt%)**	**Sulfate ERC 1 (μmol/g)**	**Sulfate ERC 2 (μmol/g)**
CNC (aq) ref	0.8839	166.99	192.71
CNC (aq) EtOH	0.3322	189.64	219.49
CNC (aq) post-heating	0.9718	179.37	200.03

Comparing the sulfate content no desulfation seems to occur. However, the dry weight of CNC treated with EtOH is quite low considering that the initial CNC suspension was of 1 wt%.

5.4 FT-IR of CNC films

CNC films were cast after hydrolysis reactions in Acetate at 37 °C. The films were used for FT-IR measurements. The data was normalized by subtracting the minimum transmittance from each transmittance value and dividing the result by the difference between the maximum and minimum transmittance value. T0* represents CNC prior to hydrolysis, whereas To/n sulf has been treated with sulfatase and To/n ref* was used to monitor the autohydrolysis, see Figure 5.13. The peak at wavenumber 815 cm^{-1} represents sulfate half esters and the transmittance at this wavenumber indicate that T0* has a higher amount of sulfate half esters than the other films. To/n sulf and To/n ref* are close in transmittance at 815 cm^{-1}, which

would suggest that they have the same amount of sulfate groups. Furthermore, it indicates that autohydrolysis is as effective as enzymatic hydrolysis for desulfation in Acetate buffer at 37 °C. However, the obtained sulfate content from conductometric titration for the same CNC dispersions implies a difference in To/n sulf and To/n ref*, see Table 5.3.

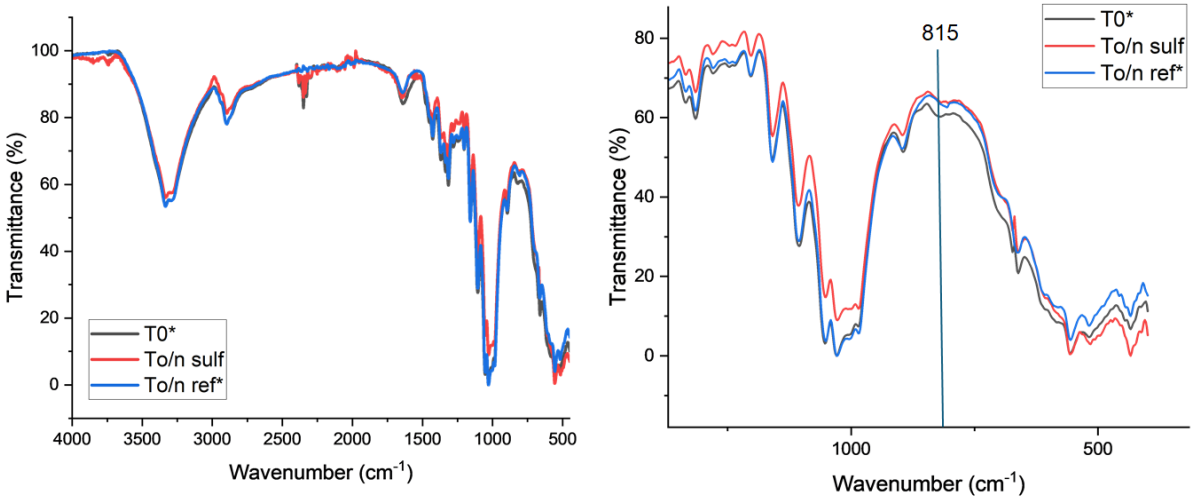

Figure 5.13: FT-IR of CNC films cast prior to hydrolysis (T0*), overnight after hydrolysis using sulfatase (To/n sulf) and overnight efter autohydrolysis (To/n ref*) in Acetate at 37 °C.

The hypothesis was that upon desulfation, the sulfate group is replaced by a hydroxyl group. To evaluate this theory the difference in intensity at the peak representing this hydroxyl group was compared. The peak for the hydroxyl group can be seen at wavenumber 3300 cm^{-1}, see Figure 5.14. It seems as though there is a lower amount of hydroxyl groups upon enzymatic desulfation (To/n sulf). However, it should be considered that CNC suspended in Acetate buffer has a sodium counterion and that these dispersions later were protonated. Therefore, it is possible that the films have different counerions affecting the measurements, making them inconclusive. In addition, the CNC moisture content from absorption/desorption of water might also affect the infrared spectra [22].

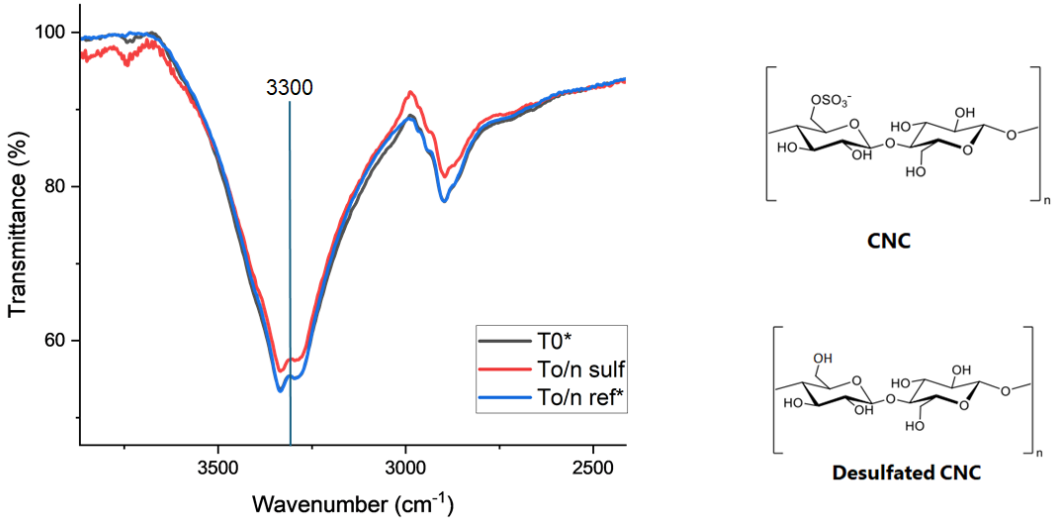

Figure 5.14: FT-IR of CNC films cast prior to hydrolysis (T0*), overnight after hydrolysis using sulfatase (To/n sulf) and overnight efter autohydrolysis (To/n ref*) in Acetate at 37 °C.

5.5 SEM images of CNC films

CNC films were cast after reactions in Acetate at 37 °C. The films were used to scan the surface with SEM. The film from suspension T0*, treated with Acetate buffer, is displayed in Figure 5.15.

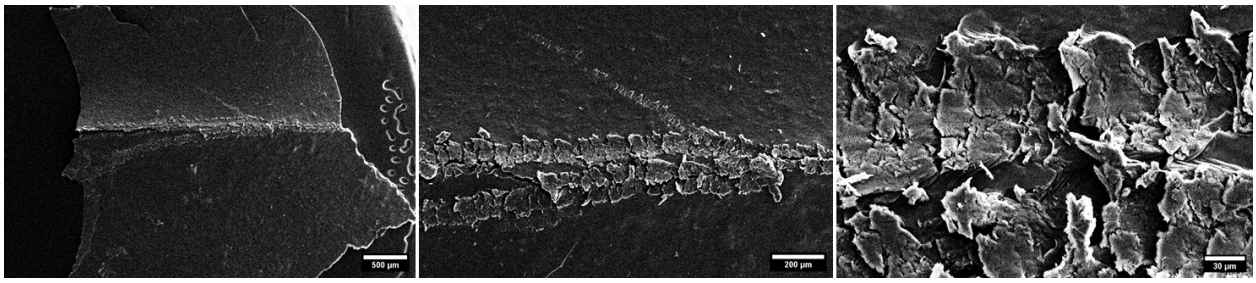

Figure 5.15: SEM images of a CNC film, cast after treatment with Acetate buffer. The magnifications from left to right are: 58X, 178X and 931X.

A film cast from CNC dispersion To/n ref*, treated with Acetate buffer and used to monitor the autohydrolysis overnight, can be seen in various magnification in Figure 5.16.

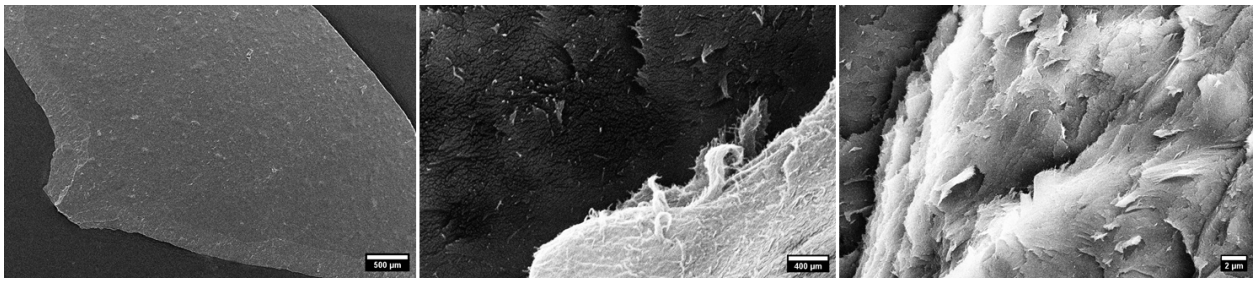

Figure 5.16: SEM images of a CNC film, cast after treatment with Acetate buffer and autohydrolysis at 37 °C overnight. The magnifications from left to right are: 58X, 8.18X and 66.1kX.

In Figure 5.17 the film cast from suspension To/n sulf is shown, i.e. CNC treated with Acetate and sulfatase overnight.

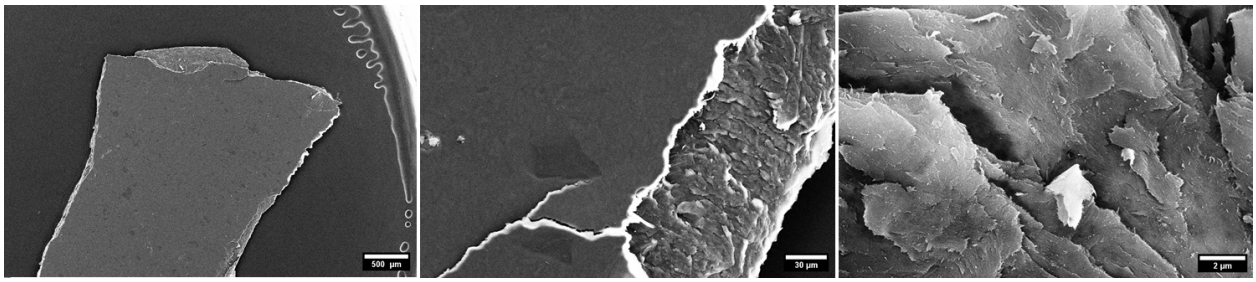

Figure 5.17: SEM images of a CNC film, cast after treatment with Sulfatase and Acetate buffer at 37 °C overnight. The magnifications from left to right are: 58X, 922X and 15.4kX

Comparing the surfaces from film To/n ref* and To/n sulf at the lowest magnification, the surface of the To/n sulf film might be smoother but it also has some darker spots. These spots may be thinner parts of the film, letting the carbon tape shine through. Looking at the same films at higher magnifications there might be some difference in how the cellulose crystallites are formed but that would have to be investigated further.

6
Conclusion

A protocol for the desulfation of CNC using sulfatase from *Helix pomatia* was developed. To monitor the activity and inhibition of sulfatase UV-Vis spectroscopy was used, where the activity was negligible after the enzyme suspension had been heated at 80 °C for 5 min. The sulfate half-ester content on the CNC surface was determined with conductometric titration after CNC had been hydrolysed for various amounts of time. There was no decrease in the sulfate content after hydrolysis (37 °C) when the CNC had been dispersed in Tris buffer (pH 7.4) , which probably was a result of a strong coordination of Tris to sulfate on the CNC surface. When CNC was suspended in Acetate buffer (pH 6.2) and hydrolysed at 37 °C it resulted in a more prominent desulfation of the CNC treated with sulfatase than the reference monitoring the autohydrolysis. To alter the selectivity of sulfatase on the CNC surface to gain further insight of the different reactivities of the sulfate groups, hydrolysis reactions were performed at RT (22 °C). This however resulted in a strong autohydrolysis, which could be explained by the fact that the Acetate buffer in these reactions had a pH of 7 that may have caused alkaline desulfation. This indicates that a lower buffer pH, around 6, may be preferable to avoid autohydrolysis, even though sulfatase has a higher activity at pH≈7. Therefore, the protocal should be optimized regarding buffer pH, temperature and sulfatase concentration. CNC films were cast after treatment with Acetate buffer (pH 6.2) and hydrolysis reactions at 37 °C. The films were used for FT-IR and SEM characterization, these results were however inconclusive. Further examination is needed, e.g. using environmental SEM to study the binding of sulfatase to the CNC surface in solution, upon hydrolysis bind a metal ion to the remaining sulfate groups for characterisation using TEM, analyse the molecular components increase/decrease upon desulfation using X-Ray diffraction.

Bibliography

[1] Lagerwall, J., Schütz, C., Salajkova, M. et al. (2014) Cellulose nanocrystal-based materials: from liquid crystal self-assembly and glass formation to multifunctional thin films. *NPG Asia Mater*, 6, e80. https://doi.org/10.1038/am.2013.69

[2] George, J., Sabapathi, S.N. (2015) Cellulose nanocrystals: synthesis, functional properties, and applications. *Nanotechnol Sci Appl*, Nov 4;8:45-54. https://doi:10.2147/NSA.S64386. PMID: 26604715; PMCID: PMC4639556.

[3] Nero M, Ali H, Li Y, Willhammar T. (2024) The Nanoscale Ordering of Cellulose in a Hierarchically Structured Hybrid Material Revealed Using Scanning Electron Diffraction. *Small Methods*, May;8(5):e2301304. https://doi:10.1002/smtd.202301304. Epub 2023 Dec 10. PMID: 38072622.

[4] Beck, S., Bouchard, J., (2014) Auto-catalyzed acidic desulfation of cellulose nanocrystals. *Nordic Pulp and Paper Research Journal*, 29(1), 006–014. https://doi:10.3183/npprj-2014-29-01-p006-014

[5] Elazzouzi-Hafraoui, S., Nishiyama, Y., Putaux, J.L., Heux, L., Dubreuil, F., Rochas, C., (2008). The shape and size distribution of crystalline nanoparticles prepared by acid hydrolysis of native cellulose. *Biomacromolecules*, Jan;9(1):57-65. https://doi:10.1021/bm700769p. Epub 2007 Dec 4. PMID: 18052127.

[6] Channab, B.E., El-Idrissi, A., Essamlali, Y., Zahouily, M. (2024). Nanocellulose: Structure, modification, biodegradation and applications in agriculture as slow/controlled release fertilizer, superabsorbent, and crop protection: A review, *Journal of Environmental Management*, Volume 352, 119928, ISSN 0301-4797, https://doi.org/10.1016/j

[7] Jordan, J.H., Easson, M.W., Condon, B.D. (2019) Alkali Hydrolysis of Sulfated Cellulose Nanocrystals: Optimization of Reaction Conditions and Tailored Surface Charge. *Nanomaterials (Basel)*, Aug 30;9(9):1232. https://doi:10.3390/nano9091232 PMID: 31480286; PMCID: PMC6780348.

[8] Yu, M., Wu, M., Secundo, F., Liu, Z. (2023) Detection, production, modification, and application of arylsulfatases, *Biotechnology Advances*, Volume 67, 108207, https://doi.org/10.1016/j.biotechadv.2023.108207

[9] Zhao, K., Liu, Z., Zhang, J., et al. (2022). Property of arylsulfatase and β-glucuronidase extracted from digestive tracts of *Cipangopaludina chinensis* and their cleavage performance on conjugated natural estrogens. *Environmental Science and Pollution Research*, 29, 64244–64251. https://doi.org/10.1007/s11356-022-22260-0

[10] Correia, Mário S.P.; Ballet, Caroline; Meistermann, Hannes; Conway, Louis P.; Globisch, Daniel (2019). Comprehensive kinetic and substrate specificity

analysis of an arylsulfatase from Helix pomatia using mass spectrometry. *Bioorganic & Medicinal Chemistry*, (), S0968089618320303–. https://doi:10.1016/j.bmc.2019.01.031

[11] Deng, Hao-Hua; Peng, Hua-Ping; Huang, Kaiyuan; He, Shao-Bin; Yuan, Qiao-Feng; Lin, Zhen; Chen, Ruiting; Xia, Xing-Hua; Chen, Wei (2019). Self-Referenced Ratiometric Detection of Sulfatase Activity with Dual-Emissive Urease-Encapsulated Gold Nanoclusters. *ACS Sensors*, (), acssensors.8b01130–. doi:10.1021/acssensors.8b01130

[12] Yang, B., Bhattacharyya, S., Linhardt, R., Tobacman, J. (2012). Exposure to common food additive carrageenan leads to reduced sulfatase activity and increase in sulfated glycosaminoglycans in human epithelial cells. *Biochimie*, 94(6), 1309-1316. https://doi.org/10.1016/j.biochi.2012.02.031.

[13] Hanson, S. R., Best, M. D., Wong, C. H. (2004). Sulfatases: structure, mechanism, biological activity, inhibition, and synthetic utility. *Angewandte Chemie International Edition*, 43(43), 5736-5763. https://doi.org/10.1002/anie.200300632. PMID: 15493058.

[14] Kaliva, M., Vamvakaki, M. (2020) Chapter 17 - Nanomaterials characterization, *Polymer Science and Nanotechnology*, Elsevier, Pages 401-433, https://doi.org/10.1016/B978-0-12-816806-6.00017-0.

[15] Khalid, K., Ishak, R., Chowdhury, Z.Z. (2024) Chapter 15 - UV–Vis spectroscopy in non destructive testing, *Non-Destructive Material Characterization Methods*, Elsevier, Pages 391-416, https://doi.org/10.1016/B978-0-323-91150-4.00021-5.

[16] NicDaéid, N. (2019) Forensic Sciences | Systematic Drug Identification, *Encyclopedia of Analytical Science (Third Edition)*, Academic Press, Pages 75-80, https://doi.org/10.1016/B978-0-12-409547-2.14457-9.

[17] Labib, M.E., Robertson, A.A., (1980) The conductometric titration of latices, *Journal of Colloid and Interface Science*, Volume 77, Issue 1, Pages 151-161, https://doi.org/10.1016/0021-9797(80)90426-9.

[18] Tideland, H., Feldhusen, J., Sonker, A.K, Westman, G. (2023) Bendable transparent films from cellulose nanocrystals–Study of surface and microstructure-property relationship, *Carbohydrate Polymer Technologies and Applications*, Volume 6, 100367, https://doi.org/10.1016/j.carpta.2023.100367.

[19] Jafari, S.M., Esfanjani, A.F., Katouzian, I., Assadpour, E. (2017) Chapter 10 - Release, Characterization, and Safety of Nanoencapsulated Food Ingredients, *Nanoencapsulation of Food Bioactive Ingredients*, Academic Press, Pages 401-453, https://doi.org/10.1016/B978-0-12-809740-3.00010-6.

[20] Perez Gutierrez, R.M., Mendez, J.V., Vazquez, I.A. (2017) Chapter 2 - A novel approach to the oral delivery of bionanostructures for systemic disease, *Micro and Nano Technologies*, Nanostructures for Oral Medicine, Elsevier, Pages 27-59, https://doi.org/10.1016/B978-0-323-47720-8.00002-X.

[21] Duchesne, I., Daniel, G. (1999). The ultrastructure of wood fibre surfaces as shown by a variety of microscopical methods - a review. *Nordic Pulp and Paper Research Journal*, 14(2), 129–139. https://doi:10.3183/npprj-1999-14-02-p129-139.

[22] Cichosz, S., Masek, A., (2020). IR Study on Cellulose with the Varied Moisture Contents: Insight into the Supramolecular Structure. *Materials*, 13(20), 4573–. https://doi:10.3390/ma13204573

A

Appendix 1

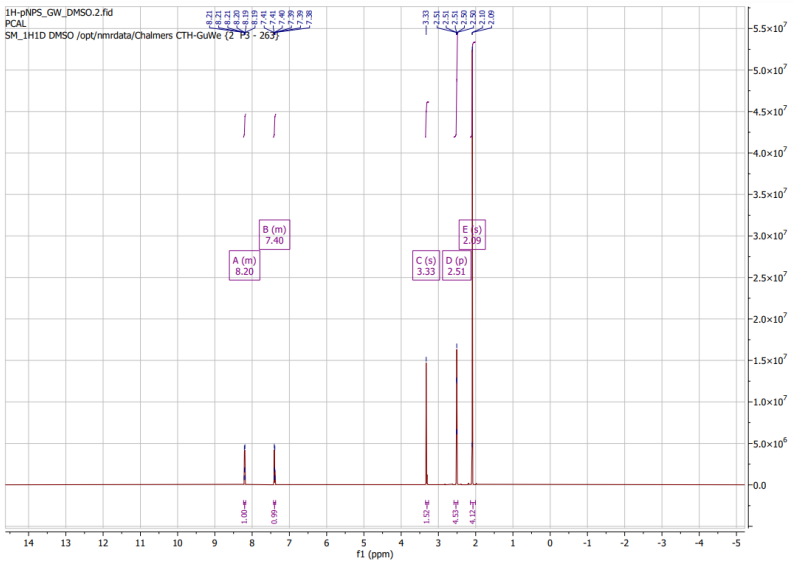

Figure A.1: ^{1}H NMR spectra of synthesized p-Nitrophenyl sulfate, solved in DMSO-d_6.

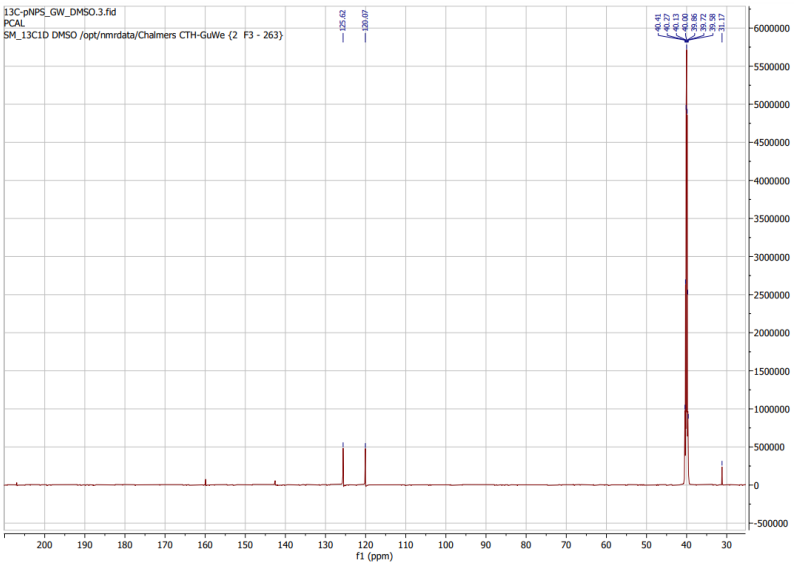

Figure A.2: ^{13}C NMR spectra of synthesized p-Nitrophenyl sulfate, solved in DMSO-d_6.

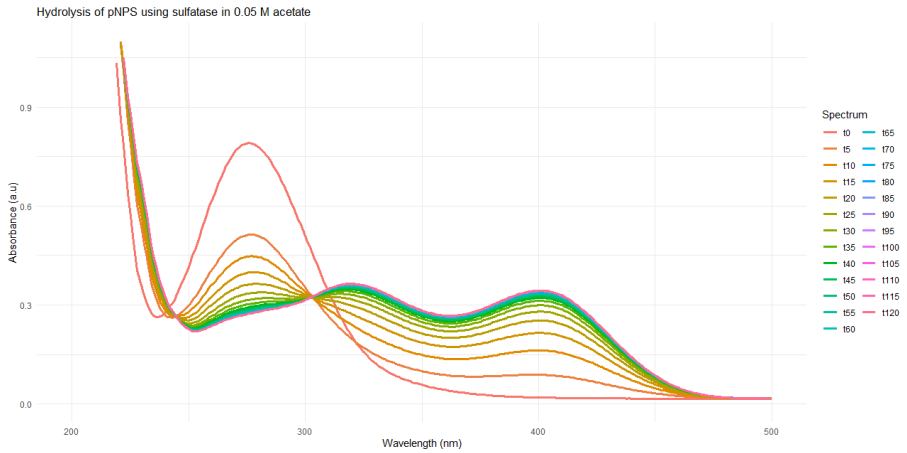

Figure A.3: UV-Vis measurement of p-Nitrophenyl sulfate and Sulfatase in 0.05 M Acetate buffer.

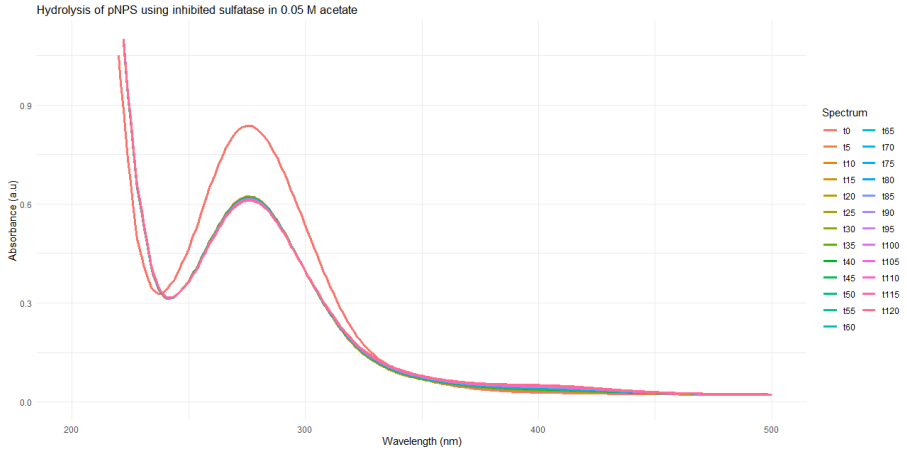

Figure A.4: UV-Vis measurement of p-Nitrophenyl sulfate and Sulfatase in 0.05 M Acetate buffer after heating.

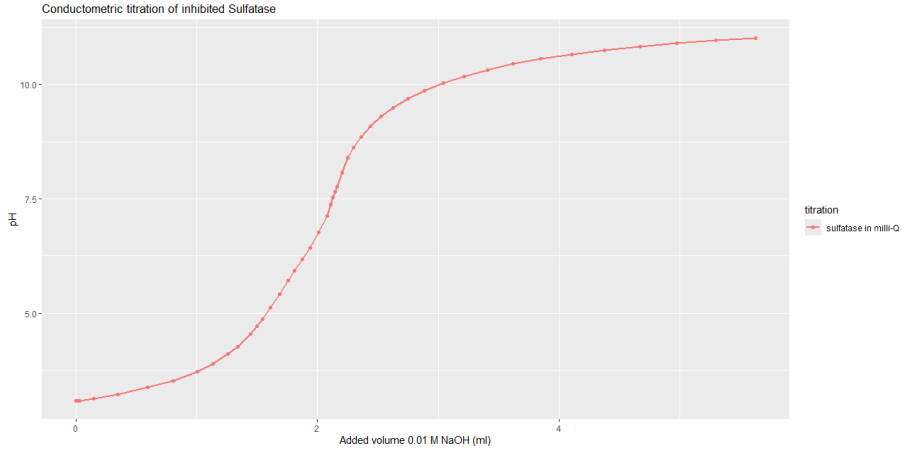

Figure A.5: Titration of sulfatase in milli-Q.

DEPARTMENT OF SOME SUBJECT OR TECHNOLOGY
CHALMERS UNIVERSITY OF TECHNOLOGY
Gothenburg, Sweden
www.chalmers.se

CHALMERS
UNIVERSITY OF TECHNOLOGY